Three-phase equilibrium and partitioning calculations for CO_2 sequestration in saline aquifers

R. C. Fuller,[1] J. H. Prevost,[1] and M. Piri[1,2]

Received 8 January 2005; revised 28 October 2005; accepted 10 March 2006; published 20 June 2006.

[1] We show how the use of appropriate variables results in a flash calculation that uses only equilibrium constraints; it is thus not necessary to solve the mass balance equations self-consistently with the equilibrium equations. We use this implicit material balance in flash calculation. We show its advantages over the current approach that uses an explicit material balance. For the flash calculation for CO_2 storage in brine aquifers, use of appropriate variables also allows us to find the dew, bubble, and precipitation points where the liquid, vapor, and solid salt phases, respectively, emerge. Our calculation includes the water content of the vapor phase, which arises from evaporation of the brine. Evaporation leads to increased brine salinity, which results in a large reduction in CO_2 solubility in the salting-out effect, and eventually in precipitation of solid salt and ultimately the disappearance of the liquid phase. The flash calculation also relies on our derivation of fugacities for H_2O and CO_2 in both the brine and the vapor phase.

Citation: Fuller, R. C., J. H. Prevost, and M. Piri (2006), Three-phase equilibrium and partitioning calculations for CO_2 sequestration in saline aquifers, *J. Geophys. Res.*, *111*, B06207, doi:10.1029/2005JB003618.

1. Introduction

[2] To determine the feasibility of deep aquifer sequestration, it is necessary to have a numerical model that can accurately predict the fate of CO_2 under the conditions of interest. A typical CO_2 storage study involves four different phase arrangements, gas/solid, gas/aqueous/solid, gas/aqueous and aqueous. The gas/aqueous/solid and gas/aqueous phase arrangements require non trivial flash calculation. We introduce an approach where the equilibrium equations alone are sufficient to define the solution for any set of phases; within our calculational scheme it is not necessary to concurrently consider material balance. Our approach tends to reduce flash calculation's contribution to the computational load of a reservoir simulation. More importantly it provides a simpler conceptual framework for the consideration of not only different phase regions, but also for the boundaries between these regions.

[3] Local equilibrium is generally assumed in reservoir calculations. Transport calculation provides the mixture component mole fractions for the input to a flash calculation which partitions these components into equilibrium phases. For CO_2 storage in deep aquifers the minimal set of components is CO_2, H_2O, and NaCl. Generally supercritical CO_2 is injected into a reservoir whose pressure and temperature assure a vapor phase whose dominant CO_2 component remains supercritical, and hence only a single H_2O-rich liquid phase results.

[4] We do not discuss reservoir simulation in this paper. However, we show results from previous work [*Prevost et al.*, 2004] in order to illustrate the evolution of fluid conditions in a reservoir that arise from water evaporation. Results shown in Figure 1 present simulation of radial injection of supercritical CO_2 into 15 wt % salinity brine at temperature = 60°C in a reservoir at pressure = 100 bar with radius = 4000 m, height = 100 m, porosity = 0.1 and absolute permeability = 100 mdarcy. CO_2 was injected at the rate of 100 kg/s.

[5] Figure 1 shows the mass fractions of CO_2 and H_2O in the liquid phase. They have been plotted versus the appropriate scaling variable ($R/\sqrt{t}$) that consolidates effects of both distance from the injection well and the time from injection onset. Injection occurs at the left moving away from the well along the radial direction. Initially there is no liquid phase; all the water in the brine has been taken up by injected CO_2 in the vapor phase and transported outward. Any existing salt has precipitated as a solid phase. Further out the vapor is saturated with water and a liquid phase appears. Now there are three coexisting phases; a CO_2-rich vapor phase, assumed to be salt free, a brine saturated with CO_2 and salt, and the solid salt phase. For three phases with three components we expect, on general grounds to be discussed later, to see what Figure 1 shows: concentrations within the phases are constant, neglecting the minor pressure effects. Moving further outward through this region, the fraction of water in the reservoir increases, and more salt is dissolved in the brine until no solid phase remains. With two phases, the mass fractions of the three components can vary. Evaporation declines, the liquid salinity decreases, and over the region where this occurs the fraction of dissolved CO_2 increases. This is simply the salting-out effect on CO_2 dissolution; higher brine salinity results is less absorbed

[1]Department of Civil and Environmental Engineering, Princeton University, Princeton, New Jersey, USA.
[2]Now at Department of Chemical and Petroleum Engineering, University of Wyoming, Laramie, Wyoming, USA.

0148-0227/06/2005JB003618$09.00

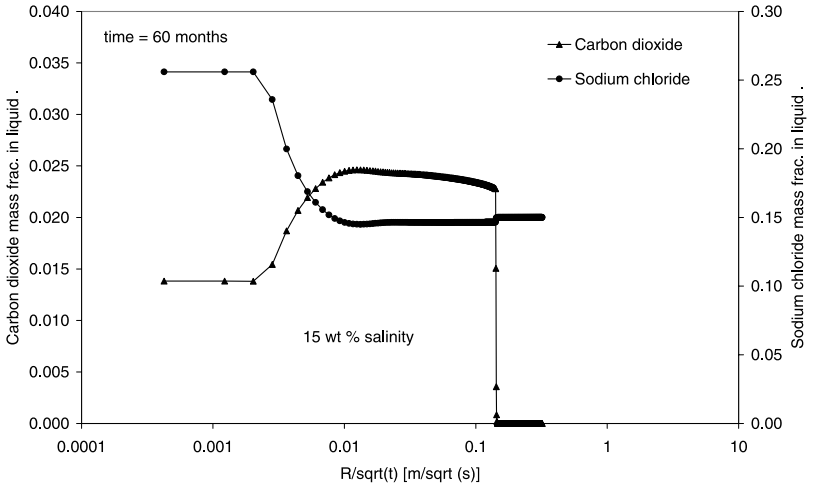

Figure 1. Reservoir simulation results of the dependence of the mass fractions of H_2O and CO_2 in the brine (we used customary variable ($R/\sqrt{t}$)).

CO_2. Finally evaporation ceases because the CO_2 rich vapor phase is fully water saturated, and the salt and CO_2 saturations level off until the limit of the CO_2 front is reached and the vapor phase vanishes. The objective of this paper is to provide flash calculation for each of these phase arrangements, which takes pressure, temperature, and mixture component mole fractions, and efficiently produces phase compositions and saturations. These are needed by the transport module in a reservoir modeling calculation that assumes there is a local thermodynamic equilibrium between the phases.

[6] In a flash calculation different equations and different variables apply within the ranges of composition that produce different sets of phases. The flash calculation must first find the phase boundaries; e.g., the flash calculation must find the input component concentrations where a single liquid phase just becomes supersaturated and an equilibrium vapor phase emerges, the so-called "bubble point." Predicting these boundaries is generally the most difficult, and problematic, aspect of flash calculation. In a sense it is necessary to perform an inverse flash calculation to locate input values corresponding to an output phase configuration before performing the forward calculation of the output for the given input.

[7] A second and related difficulty in flash calculation is the entanglement of the equilibrium calculation of component mole fractions in the equilibrium phases and the calculation of partitioning among the phases. This difficulty vanishes when the number of phases equals the number of components. In the general case, the so-called "yield factor" mole fractions [*Castier et al.*, 1989] provide variables that lead to separation of the equilibrium and partitioning calculations, even when the numbers of components and phases are not equal. Yield factor mole fractions are the fractions of the total feed of specific components that go into particular phases.

[8] Using the properties of the three-phase region, it is a simple matter to calculate the dew and precipitation point input concentrations. The bubble point is at a boundary of the liquid-vapor two-phase region. With yield factors at the bubble point, the two-phase equilibrium calculation is turned around to calculate the bubble point input concentrations as shown hereafter.

[9] For the analysis of the carbon sequestration, we derive fugacities for CO_2 and H_2O in both liquid and vapor phases. They incorporate the effects of the interaction with NaCl, whose solid phase arises from precipitation at the saturation limit of the brine.

[10] An illustrative calculation for a single flash chamber NaCl concentration, and the full range of CO_2 and H_2O flash chamber concentrations, is provided. The calculation encounters the full range of phase possibilities.

2. Variables and Flash Calculation

[11] The input to a flash calculation consists of the mole numbers of all the participating components, n_i ($i = 1, 2, \ldots, m$). Since the results cannot depend on $n = \sum_i n_i$, the input can be taken as the set, Z, of mixture component mole fractions, $Z = \{Z_i = n_i/n\}$. Further, it is to be noted that the set Z of mixture components are the natural variables which appear in the transport equations for compositional simulations [*Young and Stevenson*, 1983].

[12] A flash calculation takes the input Z and produces the distribution of components, both within phases in terms of the phase component mole fraction (PCMF) values, and among phases in terms of phase mole fraction (PMF) values. The PCMF value for component i in phase α ($\alpha = 1, 2, \ldots, \pi$), $x_{i\alpha}$, is defined by $x_{i\alpha} \equiv n_i^\alpha/n^\alpha$, where n_i^α is the number of moles of component i in phase α, and n^α is the total number of moles of all components in phase α, $n^\alpha = \sum_i n_i^\alpha$. The PMF value for phase α is $\Lambda^\alpha \equiv n^\alpha/n$. The PCMF variables are the variables traditionally referred to as simply "mole fractions." Since much of our work depends on distinctions between different types of mole fractions, we state the significance of PCMF variables: they describe the molar fraction of a phase that consists of a given component and this is why we refer to them as phase component mole fractions. Our notation conventions are discussed in Appendix A.

[13] In a flash calculation, the constraints fall into two classes: one to describe the equilibrium component con-

centration within phases, and a second to describe the partitioning of the available components among the phases. Variables fall into two parallel classes: one, the previously defined PCMF variables, refer to component concentrations within phases; and a second, the yield factor mole fractions (YFMF) [*Castier et al.*, 1989] defined by $\lambda^{\alpha i} \equiv n_i^\alpha/n_i$, which describe partitioning of the components among the phases. Because these variables could be confused with the PCMF mole fractions we state their significance: they describe the molar fraction of a component in a given phase.

2.1. Phase Equilibrium Constraints

[14] Equilibrium between the phases at fixed pressure and temperature requires equality of the chemical potentials for all the phases for each component i

$$\mu_i^1 = \mu_i^2 = \ldots = \mu_i^\pi \qquad (i = 1, 2, \ldots, m) \tag{1}$$

where μ_i^α at fixed pressure and temperature depends only on $x_\alpha \equiv \{x_{i\alpha}\}$, the set of $x_{i\alpha}$ for all the components in phase α:

$$\mu_i^\alpha = \mu_i^\alpha(x_\alpha) \tag{2}$$

2.2. Component and Phase Partitioning

[15] Flash calculation must satisfy the partitioning constraints along with equilibrium constraints. Partitioning can be expressed either as partitioning a component among phases or a phase among components, again reflecting the duality between components and phases. The relationship between these two modes of partitioning follows from expressing n_i^α/n as either $(n_i^\alpha/n^\alpha)(n^\alpha/n) = x_{i\alpha}\Lambda^\alpha$ for partitioning a phase among components or as $(n_i^\alpha/n_i)(n_i/n) = \lambda^{\alpha i} Z_i$ for partitioning a component among phases. The equivalence of the two modes is expressed by

$$x_{i\alpha}\Lambda^\alpha = \lambda^{\alpha i} Z_i \tag{3}$$

which holds for each α and each i. There is no implied summation over repeated indices in any of the equations in this paper. Summing equation (3) over phases, α, and in turn over components, i, and using $\sum_i x_{i\alpha} = 1$ and $\sum_\alpha \lambda^{\alpha i} = 1$ yields the two partitioning equations

$$Z_i = \sum_\alpha x_{i\alpha}\Lambda^\alpha \tag{4}$$

and

$$\Lambda^\beta = \sum_i \lambda^{\beta i} Z_i \tag{5}$$

Equation (4) expresses the partitioning of the PMF, Λ, by the x_i into the input Z_i, while equation (5) expresses the dual relation, partitioning Z by λ^β into the output Λ^β. At this stage we have two separate ways to express partitioning. Flash calculation must satisfy these expressions along with the equilibrium constraints.

[16] Equation (4) is generally referred to as the mass balance equation. Both equations (4) and (5) express a molar partitioning relationship between phases and components, and we have referred to their use as partitioning.

2.3. Integrating Equilibrium Constraints and Partitioning

[17] Here we verify that the equations to be solved are equal in number with the variables used in the flash calculation.

2.3.1. Flash Calculation With PCMF Variables

[18] The number of equilibrium constraints, N_E, in equation (1) is

$$N_E = m(\pi - 1) \tag{6}$$

Since $\sum_i x_{i\alpha} = 1$ the number of independent PCMF variables in the set x is

$$N_x = \pi(m - 1) \tag{7}$$

If we consider the equilibrium constraints alone, along with the x variables to express them, then $N_E - N_x = -m + \pi$, and we reach one of the following conclusions:

[19] 1. For $m = \pi$, the component concentrations within phases are given by the equilibrium equations alone; i.e., they do not depend on Z; only the relative amounts of different phases, given by Λ^α, depends on the input Z through equation (4). With the equilibrium x, the resulting square matrix in equation (4) can be inverted to yield Λ as

$$\Lambda = x^{-1} Z \tag{8}$$

[20] 2. For $m \neq \pi$, the equilibrium equations, (equation (1)), and the partitioning equations (equation (4)), must be solved concurrently for x and Λ. Since $\sum_\alpha \Lambda^\alpha = 1$ the number of independent Λ variables is

$$N_\Lambda = \pi - 1 \tag{9}$$

and since $\sum_i Z_i = 1$ the partitioning equations (equation (4)), contribute

$$N_Z = m - 1 \tag{10}$$

equations. From equations (6), (7), (9), and (10), the relation $N_E + N_Z = N_x + N_\Lambda$ follows. Therefore the concurrent solution of equations (1) and (4) can provide the flash solution for x and Λ. The need for concurrent solution reflects the coupling of the internal phase composition given by x and the input Z through equation (4).

2.3.2. Flash Calculation With YFMF Variables

[21] Since the equilibrium constraints in equation (1) are expressed in terms of the PCMF variables, x, it is first necessary to express x in terms of the YFMF variables λ. Using equation (5) in equation (3), and solving for $x_{i\alpha}$ yields the desired relation

$$x_{i\alpha} = \frac{\lambda^{\alpha i} Z_i}{\sum_j \lambda^{\alpha j} Z_j} \tag{11}$$

Substitution for the x variables in equation (1) provides equilibrium equations that depend only on λ and Z; that is,

instead of $\mu_i^\alpha(x_\alpha)$ we have $\mu_i^\alpha(\lambda^\alpha, Z)$. The equilibrium equations now contain the input data, and they provide enough constraints to give the YFMF solution; since $\sum_\alpha \lambda^{\alpha i} = 1$, the number of independent λ variables is

$$N_\lambda = m(\pi - 1) \tag{12}$$

and hence $N_E = N_\lambda$. The complete flash solution now follows: the λ are solutions of the equilibrium equations (equation (1)), and then Λ^α and $x_{i\alpha}$ are given by evaluation of equations (5) and (11), respectively.

2.3.3. The Reason to Use YFMF Variables

[22] To this point, the discussion has been abstract. It is useful to understand the significance of the use of YFMF, or λ, variables: they incorporate within themselves the constraints of material balance. When $m \neq \pi$, equilibrium cannot be determined by equilibrium constraints between phases alone; equilibrium generally must include consideration of the overall component composition of the mixture. The traditional approach [*Prausnitz et al.*, 1999; *Firoozabadi*, 1999; *Smith et al.*, 1996] uses PCMF variables in the phase equilibrium portion of the calculation, and introduces the effects of the overall composition with separate but coupled material balance equations.

[23] With λ variables, material balance is incorporated within the expression of the PCMF, or x, variables given by equation (11). This provides for closure of the equilibrium equations alone, which now depend on the component composition through the input Z, and on the component partitioning among phases through the λ variables.

[24] Consideration of brine and a coexisting vapor phase provides a useful physical picture of the need for material balance in an equilibrium calculation, i.e., how the composition of the aqueous brine and vapor phases depends on the relative quantities of salt, water, and CO_2 available for equilibration. In the absence of a solid phase, the aqueous phase is not salt saturated. When additional water is made available, the aqueous phase is generally diluted, but then the brine can dissolve more CO_2 in the reverse of the salting out effect, and then there is less CO_2 in the vapor phase. With less CO_2, the saturated vapor phase holds less water, and ever onward toward self-consistency of equilibrium and material balance.

2.4. Comments on the Phase Boundary Problem in Flash Calculation

[25] Flash calculation is performed within a region of input Z where the number of phases and their types is fixed. It is necessary to find the boundaries of these regions. For the CO_2-brine system we are able to find them outside the flash calculation itself; we do not rely on the interpretation of anomalies within calculations [see, e.g., *Nghiem et al.*, 1983] that include material balance.

[26] For the CO_2-brine system, three phases coexist when the brine phase is saturated with salt. The region of inputs that support three phases is easy to find. We have argued that the PCMF values are constant within this region. With the constant x values it is a straightforward matter to find the Z values where particular Λ^α vanish. For the CO_2, brine, and salt system, the dew point Z corresponds to the vanishing of the liquid phase at $\Lambda^l = 0$, and the precipitation point, to the vanishing of the solid phase at $\Lambda^s = 0$, where superscripts l and s stand for liquid and solid, respectively.

[27] For this system the bubble point Z can occur at a Z value between the two-phase (vapor plus brine) and the single-phase (carbonated brine) systems, where the brine is not saturated with salt and the bubble point depends on mass balance as well as phase equilibrium. Here we reverse the usual flash calculation to solve for Z with the YFMF λ variables expressing the boundary phase condition. All this will receive further discussion in section 3.

3. CO_2 Brine Flash Calculation

[28] Our primary purpose is the description of a general approach to flash calculation when not all the phases are saturated. This is the predominant case for CO_2 sequestration in a brine reservoir. The calculation that follows is intended as a first application of the scheme. It is not intended at this stage to supersede any other approach to the calculation of fugacities. Our approach is general and can be used with any set of fugacities.

[29] The target application is reservoir simulation for CO_2 storage in deep brine aquifers where the CO_2-rich phase is supercritical, and the only liquid phase is carbonated brine. A solid salt phase can also exist. We will refer to the supercritical CO_2 rich phase as the vapor phase. Water can evaporate from the brine, leading to higher brine salinity and, in the limit, to salt supersaturation, which results in salt precipitation. The only salt we consider is Sodium Chloride (NaCl). We make the usual assumptions that the vapor contains no salt, and the solid phase is pure salt.

[30] Following standard practice [*Prausnitz et al.*, 1999], we will express the equilibrium equations (1) and (2) in terms of the fugacities $f_i^\alpha(x_\alpha)$

$$f_i^1(x_1) = f_i^2(x_2) = \ldots = f_i^\pi(x_\pi) \quad (i = 1, 2, \ldots, m) \tag{13}$$

where x_α denotes the set of $x_{i\alpha}$ for all components i in the phase α. We will generally solve for the (λ, Z) variables with $f^\alpha(\lambda^\alpha, Z)$ in equation (13); recall λ are the YFMF variables.

[31] We first discuss the YFMF and PCMF variables for CO_2 storage in brine aquifers. We then derive a set of fugacity expressions for use in the component equilibrium equations, and finally discuss our flash calculation results.

[32] For three coexisting phases there are three independent variables of each variety. The simplification provided by YFMF variables becomes apparent in the flash calculation when the liquid is not saturated with salt. Now there is no solid phase, i.e., $\lambda^{l,sc} = 1$ where superscript *sc* stands for Sodium Chloride. Also, there are two independent YFMF variables, $\lambda^{l,w}$ and $\lambda^{l,c}$, where superscripts w and c stand for water and carbon dioxide, respectively, and two equilibrium equations. We solve the equilibrium equations for $\lambda^{l,w}$ and $\lambda^{l,c}$ and complete the flash calculation by straightforward evaluation of equation (5) for Λ^l and equation (11) for $x_{w,l}$, $x_{c,l}$ and $x_{w,v}$. With PCMF variables, the flash calculation requires the simultaneous solution of four coupled equations. There are three independent PCMF variables that can be taken as $x_{w,l}$, $x_{c,l}$ and $x_{w,v}$, where subscript v stands for vapor. The two equilibrium equations are insufficient, and it is necessary to augment them with two independent equa-

tions in equation (5) for two of the components, say those for Z_w and Z_c. This introduces the remaining flash calculation unknown, the liquid PMF Λ^l. It is now necessary to solve four simultaneous equations:

$$f_w^l(x_l) = f_w^v(x_v) \tag{14a}$$

$$f_c^l(x_l) = f_c^v(x_v) \tag{14b}$$

$$Z_w = \Lambda^l x_{w,l} + \left(1 - \Lambda^l\right) x_{w,v} \tag{14c}$$

$$Z_c = \Lambda^l x_{c,l} + \left(1 - \Lambda^l\right) x_{c,v} \tag{14d}$$

3.1. Equilibrium Calculations

3.1.1. Fugacities for CO_2 and H_2O

[33] Fugacities at fixed pressure and temperature follow immediately from the partial molar Gibbs free energies. We will derive expressions for the molar free energy, g^α, in phase α. For phase molar number n^α, the partial molar energy for component i in phase α, g_i^α, is

$$g_i^\alpha = \frac{\partial(n^\alpha g^\alpha)}{\partial n_i^\alpha} \tag{15}$$

and the fugacity f_i^α satisfies

$$g_i^\alpha - g_i^{\alpha,0} = RT \ln \frac{f_i^\alpha}{f_i^{\alpha,0}} \tag{16}$$

where the superscript 0 is used to denote the reference state.

[34] It is common to decompose the liquid molar free energy g^l, into contributions from the pure phases, and the excess free energy arising from interactions between different components in the liquid:

$$g^l = g^l_{\text{brine}} + g^l_c + g^l_{ex} \tag{17}$$

where g^l_{brine} and g^l_c are pure substance free energies and g^l_{ex} is the molar excess contribution; at this stage we treat brine as a pure substance.

[35] For the liquid phase we use a two-parameter Margules-like [*Prausnitz et al.*, 1999] formula for the molar dependence of the excess free energy, g^l_{ex}; which follows from the simplest expression of the molar boundary conditions for $g^l_{ex}(x_l) = 0$, $x_{\text{brine,l}} = 0$ or $x_{c,l} = 0$ with $x_{\text{brine,l}} = x_{w,l} + x_{sc,l} = 0$ if and only if both $x_{w,l} = 0$ and $x_{sc,l} = 0$ since mole fractions are positive. (In a paper that appeared after we submitted our manuscript [*Spycher and Pruess*, 2005] an even simpler approach that assumes the component fugacities are proportional to the component concentrations in the phases, what is called an ideal mixture treatment, is shown to fit the concentration data.) Consistent with enforcing these boundary conditions and retaining pressure and temperature dependence separately we have

$$g^l_{ex} = x_{c,l}\left\{x_{w,l}F_2(P,T) + x_{sc,l}F_3(P,T)\right\} \tag{18}$$

where $F_2(P, T)$ and $F_3(P, T)$ are arbitrary functions. Later they will be fit to solubility data.

Fugacity expressions use the activity coefficients:

$$RT \ln \gamma_c \equiv \frac{\partial\left(n^l g^l_{ex}\right)}{\partial n^l_c} = \left(1 - x_{c,l}\right)\left\{x_{w,l}F_2(P,T) + x_{sc,l}F_3(P,T)\right\} \tag{19}$$

and

$$RT \ln \gamma_w \equiv \frac{\partial\left(n^l g^l_{ex}\right)}{\partial n^l_w} = x_{c,l}\left\{\left(1 - x_{w,l}\right)F_2(P,T) - x_{sc,l}F_3(P,T)\right\} \tag{20}$$

The fugacities now follow as

$$f^l_c = x_{c,l} f^l_{\text{pure } c} \gamma_c \tag{21}$$

and

$$f^l_w = x_{w,l} f^l_{\text{pure } w} \gamma_w \tag{22}$$

[36] Since γ_w is calculated as a free energy in excess of CO_2 and brine, the pure water contribution should be multiplied by a factor that accounts for the excess free energy arising from the interaction of salt and water. We investigated the contribution of such a term to our fit, which will be discussed shortly. It provided no discernible improvement, and to avoid unnecessary complication, we dropped it. In principle the preferred approach would have been to evaluate the effect of the water-salt interaction in the binary brine system alone. Instead we chose the strictly pragmatic path of looking for the effect in the full brine-CO_2 system.

[37] CO_2 is supercritical, therefore $f^l_{\text{pure } c}$ is the same as a pure CO_2 vapor phase fugacity, i.e., $f^l_{\text{pure } c} = f^v_{\text{pure } c}$. For the pure liquid H_2O fugacity we make the usual Poynting correction [*Prausnitz et al.*, 1999] to the lowest order fugacity value, P_{vp}, pure water vapor pressure at P and T, to give

$$f^l_{\text{pure } w} = P_{vp} \exp\left(\frac{P - P_{vp}}{RT} v_{\text{avg}}\right) \tag{23}$$

where v_{avg} is an average H_2O molar volume. The physical interpretation of equation (23) is given by *Prausnitz et al.* [1999]. The results of our calculation are not sensitive to the assumed form of equation (23) because the fit to $F_2(P, T)$ will assure the correct overall value of the H_2O liquid fugacity.

[38] In the vapor phase the H_2O concentration is small, generally less than 0.5%. This suggests that the Raoult limit $x_{c,v} = 1$ be used to evaluate the CO_2 vapor fugacity coefficient φ^v_c, and that the complementary Henry limit $x_{w,v} = 0$ be used to evaluate the H_2O vapor fugacity coefficient, φ^v_w. Both can be obtained from an expression derived from an equation of state; we follow *Spycher et al.* [2003], then

$$f^v_c = x_{c,v} P \varphi^v_c\left(x_{c,v} = 1\right) \tag{24}$$

$$f^v_w = x_{w,v} P \varphi^v_w\left(x_{w,v} = 0\right) \tag{25}$$

where P is the flash chamber pressure. The pure CO_2 density used to evaluate the fugacity coefficients is calculated from the same modified *Redlich and Kwong* [1949] equation of state used to derive the fugacity coefficients. At supercritical conditions the pure CO_2 phase cubic EOS has only one solution which yields the density.

[39] The equilibrium constraint equations for CO_2 and H_2O in coexisting vapor and liquid phases follow from substituting equations (21)–(25) into equations (14a) and (14b):

$$x_{c,l}\gamma_c = x_{c,v} \tag{26}$$

$$x_{w,l}\left\{\frac{P_{vp}\ \exp\{[(P-P_{vp})/RT]v_{\text{avg}}\}}{P\varphi_w^v(x_{w,v}=0)}\right\}\gamma_w = x_{w,v} \tag{27}$$

Note the cancellation of the pure phase liquid and vapor CO_2 fugacity coefficients in equation (26); we are assuming that pure phase CO_2 exists only as supercritical fluid in this application.

3.1.2. NaCl Equilibrium Constraint

[40] For Z values in the three-phase sector, the liquid phase is saturated with a Z-independent NaCl concentration. We approximate the NaCl saturation concentration with its CO_2 free value; $Z_c = 0$ is not in the three-phase region, and therefore we are neglecting any dependence of dissolved CO_2 on NaCl saturation.

[41] The saturation limit in the liquid phase provides the NaCl equilibrium constraint equation

$$\frac{x_{sc,l}}{x_{w,l}} = \frac{m_{sat}(P,T)}{55.508} \tag{28}$$

where $m_{sat}(P, T)$ is NaCl saturation limit. We now have three equilibrium equations, equations (26), (27), and (28), when the input Z values are in the three-phase sector. (note that γ_c and γ_w are given by equations (19) and (20), respectively.)

3.2. Flash Calculation Scheme

[42] The flash calculation proceeds in two stages: first, calculation of quantities that only depend on the pressure, P, and temperature, T. These include the functions $F_2(P, T)$ and $F_3(P, T)$ that appear in the excess partial free energies, and the flash chamber component mole fractions at the dew, precipitation, and bubble points. The second stage is the iterative calculation with the equilibrium constraints.

[43] The current flash calculation produces F_2(P, T) and F_3(P, T) directly from the smoothed CO_2 solubility data provided by the calculation of *Duan and Sun* [2003]. Using $x_{c,v} = 1 - x_{w,v}$, equations (26) and (27) are combined into one equation that only involves the liquid mole fractions:

$$x_{c,l}\gamma_c + x_{w,l}X(P,T)\ \gamma_w = 1 \tag{29}$$

with

$$X(P,T) = \frac{P_{vp}\exp\{[(P-P_{vp})/RT]v_{\text{avg}}\}}{P\varphi_w^v(x_{w,v}=0)} \tag{30}$$

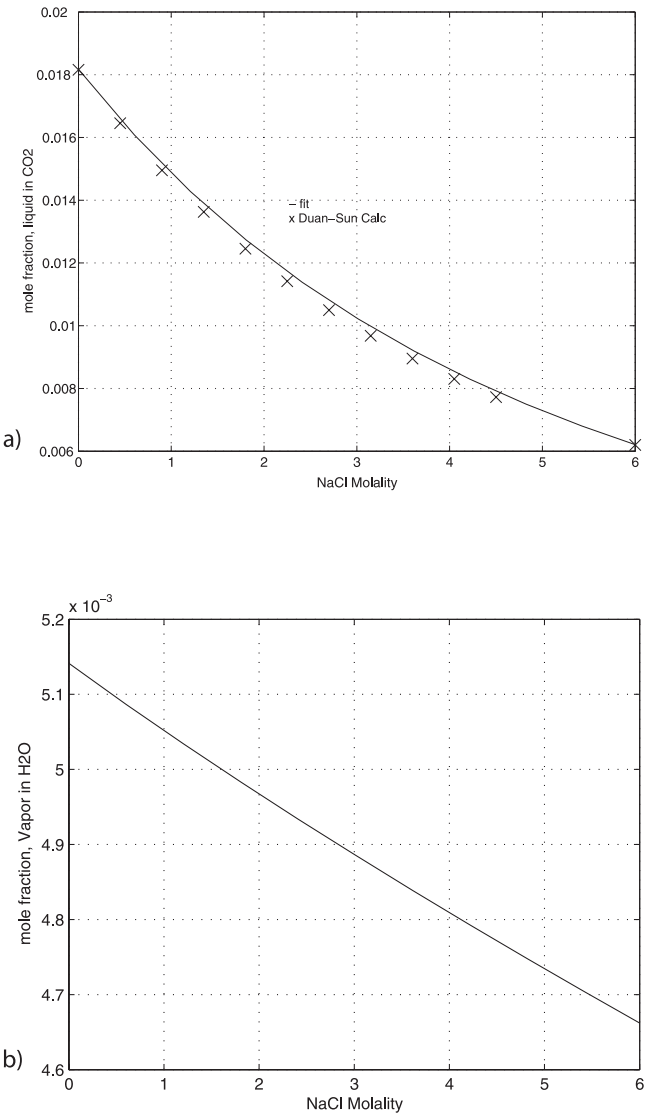

Figure 2. (a) Salting out of CO_2 from the liquid, fit compared with the calculation by *Duan and Sun* [2003] at P = 10 MPa and T = 60°C. (b) Calculated H_2O concentration in the vapor.

F_2 is found from the solution of equation (29) by setting $x_{sc,l} = 0$ at P and T and taking $x_{c,l}$ from *Duan and Sun* [2003]. With this F_2, F_3 follows by using a nonzero $x_{sc,l}$ again with $x_{c,l}$ taken from *Duan and Sun* [2003]; for the nonzero $x_{sc,l}$ we generally use the value corresponding to the NaCl saturation limit, $m_{sat}(P, T)$. With F_2 and F_3 either of equation (26) or (27) can be used to calculate the vapor mole fractions. *Duan and Sun*'s [2003] calculation provides a smoothed representation of a large fraction of available measurements.

[44] Figure 2a shows a comparison with our results of this calculation. Our calculation used F_2 and F_3 parameters that were obtained using a simple fitting scheme to two points from *Duan and Sun*'s [2003] calculation. It is reassuring that the use of results from *Spycher et al.* [2003] in the calculation of the H_2O vapor phase fugacity for pure water gives a good result when used in our calculation in the NaCl-

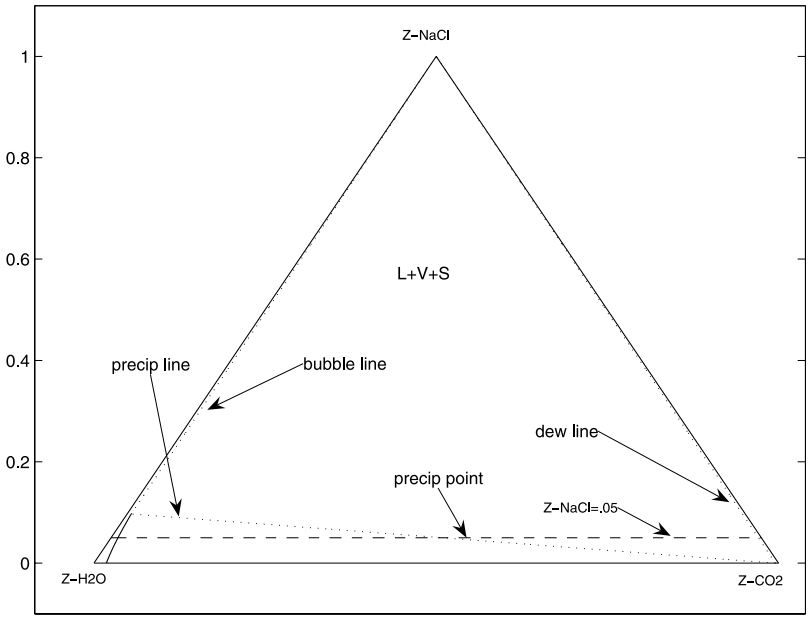

Figure 3. Ternary plot of phase structure in the space of the input flash chamber Z mole fractions. The indicated three-phase region lies within the inscribed dotted line. The horizontal dashed line is at Z-NaCl = 0.05.

free case. The H_2O concentration in the vapor varies slightly with the brine's salinity; the dependence shown in Figure 2b is a prediction since no data are available. Note that the increase in salt content in the water reduces the amount of water in the vapor. (In a recent paper, *Spycher and Pruess* [2005] presented calculations of mutual solubility of CO_2 and H_2O in brine and the coexisting vapor phases. Their calculations and ours both produce H_2O solubility in the vapor phase within the mole fraction range of 4.5×10^{-3} to 5.1×10^{-3}. Both calculations covered effectively the same salt molality range. Their work treats the aqueous phase salt molality as an independent variable. A basic conclusion of our work is that it, or equivalently the salt mole fraction, must be varied in solubility calculations. In the absence of a solid phase all the salt does reside in the aqueous phase, but the water partitioning between the aqueous and vapor phases cannot be determined by the phase compositions alone; it depends on the overall component composition. This is most significant when there is relatively little water available to the equilibrium calculation.)

4. Illustrative Calculation

[45] Our calculation shows the results of the entire range of flash calculations for fixed pressure P = 10 MPa, temperature T = 60°C, and Z_{sc} = 0.05. (We plan to make the calculation software generally available.)Capillary pressure between liquid and vapor phase is ignored. With the vapor pressure P_{vp} calculated by an algorithm taken from *Duan and Sun* [2003] and $v_{\text{avg}} = 18 \times 10^{-6}$ m^3/mol, we find F_2/RT = 4.1522 and F_3/RT = 14.2827. Our approach will first calculate the dew, precipitation, and bubble point Z values. With Z_{sc} fixed there is only one remaining degree of freedom in the Z values; we generally show variation with Z_c, but this is equivalent to variation of $Z_w = 0.95 - Z_c$, where $0 < Z_c < 0.95$.

[46] For $Z_c < (Z_c)_{\text{bubble}}$, there is insufficient CO_2 to saturate the brine, resulting in a single liquid phase of carbonated brine. For $(Z_c)_{\text{bubble}} < Z_c < (Z_c)_{\text{precip}}$, there are coexisting vapor and liquid phases; the brine is not saturated with salt. In this region the YFMF variables provide the route to a solution with the equilibrium equations alone.

[47] A third, solid NaCl phase results when $(Z_c)_{\text{precip}} < Z_c < (Z_c)_{\text{dew}}$. Here there is insufficient water to dissolve the salt, and the solid phase appears. With three phases and three components, the PCMF values do not vary with Z. They are used in equation (8) to find the PMFs Λ over the entire three-phase sector.

[48] Finally for $(Z_c)_{\text{dew}} < Z_c$, there is insufficient water to saturate the vapor, and all the CO_2 and H_2O reside in a vapor phase. We assume the NaCl resides in an uncoupled solid phase.

4.1. Dew, Precipitation, and Bubble Z

[49] In our calculation the Z boundary of the three-phase region consists of three lines; the dew line, the bubble line, and the precipitation line. The Z values at the boundary follow from the matrix equation (4) $Z = x\Lambda$, with the Λ values corresponding to a boundary. By way of example, the precipitation line corresponds to $\Lambda^s = 0$, and hence to $\Lambda^v = 1 - \Lambda^l$ with $0 < \Lambda^l < 1$. Figure 3 used Z_w = 0.4, Z_c = 0.3, and Z_{sc} = 0.3 to calculate the three-phase x matrix elements. With the rows taken in order H_2O, CO_2, and NaCl and the columns in order vapor, liquid, and solid, equation (4) for the dew line is

$$\begin{bmatrix} Z_w \\ Z_c \\ Z_{sc} \end{bmatrix} = \begin{bmatrix} 4.6621 \times 10^{-3} & 0.8968 & 0 \\ 0.9954 & 6.2111 \times 10^{-3} & 0 \\ 0 & 0.0970 & 1 \end{bmatrix} \begin{bmatrix} 1 - \Lambda^l \\ \Lambda^l \\ 0 \end{bmatrix}$$

It is now obvious that the three-phase region is a triangle in Z space with vertices at points specified by the columns of

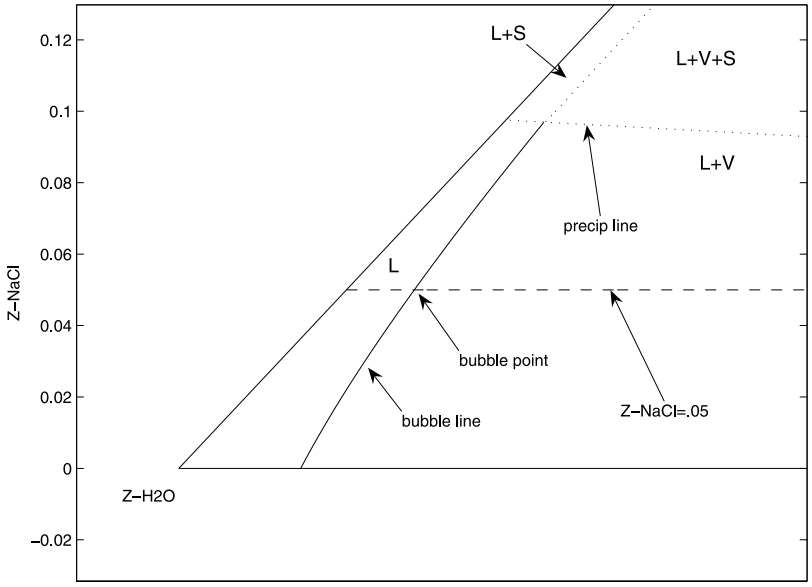

Figure 4. Magnified view of the bubble region in the ternary plot. The bubble point on the curved bubble line lies between the liquid plus vapor and the pure liquid phase regions.

the x matrix. Figure 3 shows a ternary plot of this triangle. It also shows the $Z_{sc} = 0.05$ line corresponding to the illustrative calculation; it intersects the precipitation line at the precipitation point $Z_c = 0.4852$ where the solid phase appears.

[50] Figures 4 and 5 show the magnified lower corners of Figure 3. Figure 4 shows the bubble line between the pure liquid and the liquid plus vapor regions. The bubble line occurs when the vapor phase vanishes from the vapor-brine system, where $\lambda^{l,w} = \lambda^{l,c} = \lambda^{l,sc} = 1$, $x_{w,l} = Z_w = (1 - Z_{sc})(1 - \zeta)$ and $x_{c,l} = (1 - Z_{sc})\zeta$, where $0 < \zeta < 1$ specifies the position on the bubble line. The bubble line ζ can now be found as a solution to equation (29). The bubble point occurs at $Z_c = 0.0101$ corresponding to $Z_w = 0.9399$. For $Z_c < 0.0101$, all the CO_2 is dissolved in the brine.

[51] Figure 5 shows the dew line where the H_2O presence becomes sufficient to saturate the vapor phase. The dew point for $Z_{sc} = 0.05$ occurs at $Z_c = 0.9456$ and hence for $Z_w < 0.0044$, all the H_2O goes into the vapor phase, and all the NaCl is in the solid phase.

4.2. Flash Calculation Solution by Sectors

[52] We now discuss the flash calculation for each phase sector.

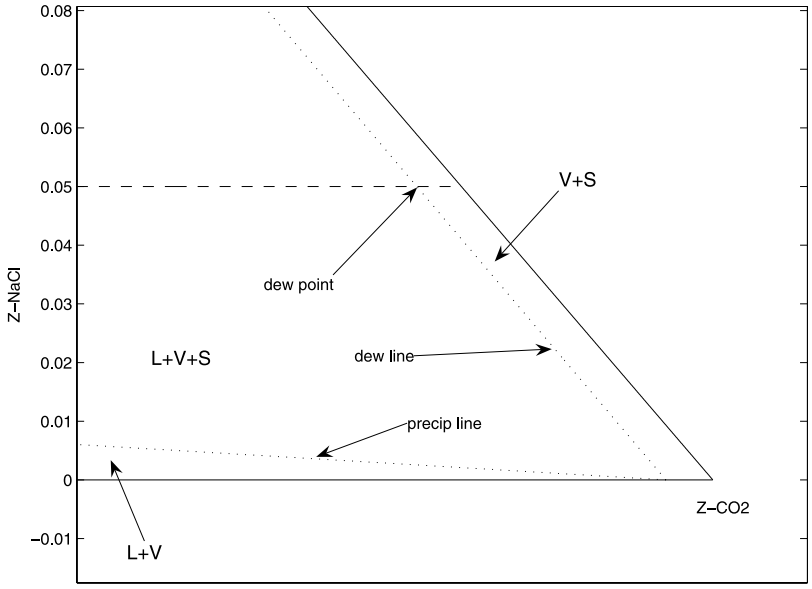

Figure 5. Magnified view of the dew region in the ternary plot. The dew point lies between the vapor plus solid and the liquid plus vapor plus solid phase regions.

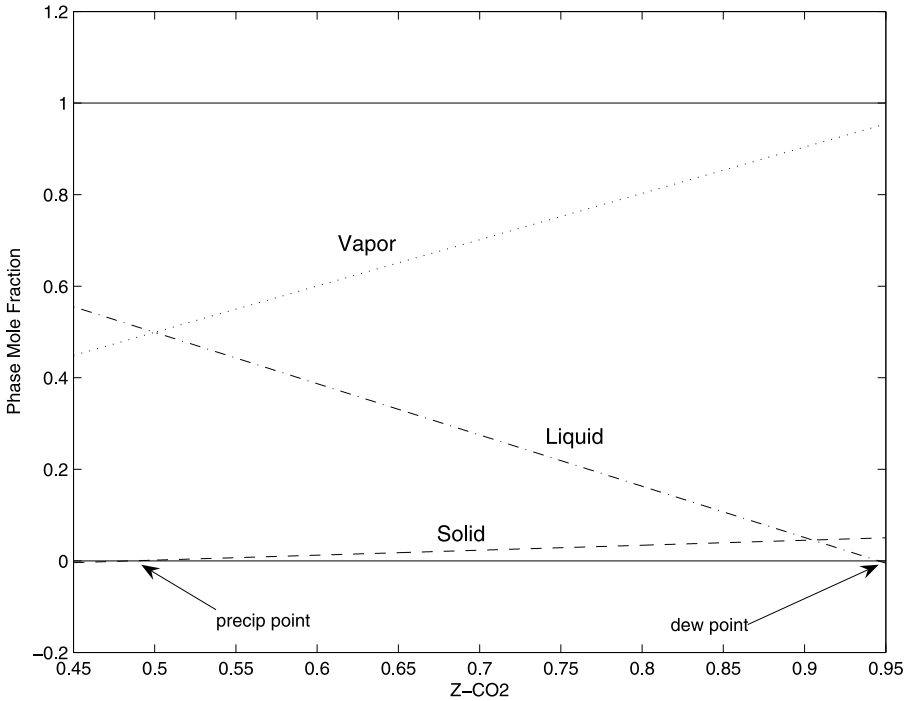

Figure 6. Three-phase region PMFs between the precipitation and the dew points.

4.2.1. Carbonated Brine Phase

[53] For $Z_c < 0.0101$, the bubble point, there is only the single phase of carbonated brine. The flash solution is

$$\Lambda^l = 1$$

$$\Lambda^v = \Lambda^s = 0$$

$$x_{w,l} = Z_w$$

$$x_{c,l} = Z_c$$

$$x_{sc,l} = Z_{sc}$$

4.2.2. Humid Vapor Plus Solid Salt

[54] For $Z_c > 0.9456$, the dew point, a humid CO_2 vapor coexists with solid NaCl. The flash solution is

$$\Lambda^l = 0$$

$$\Lambda^v = 0.95$$

$$\Lambda^s = 0.05$$

$$x_{w,v} = Z_w/(Z_w + Z_c)$$

$$x_{c,v} = 1 - x_{w,v}$$

$$x_{sc,s} = 1$$

4.2.3. Coexisting Liquid, Vapor, and Solid

[55] For Z_c between the dew and precipitation points, $0.4852 < Z_c < 0.9456$, there are three phases. Since the number of phases and the number of components are the same, and we already have the PCMF values from the dew and precipitation point calculations, the PMF, Λ, follow immediately from inverting equation (4). The values are shown in Figure 6. Since $Z_w = 1 - Z_{sc} - Z_c = 0.95 - Z_c$, the Λ^α depend linearly on Z_c.

[56] This approach to flash calculation uses the characteristics of the $m = \pi$ flash calculation, and it is practical in this instance because it is easy to guess input Z that produce a three-phase solution.

4.2.4. Humid Vapor and Carbonated Brine Phases

[57] The vapor-liquid, two-phase region occurs between the bubble and precipitation points, $0.0101 < Z_c < 0.4852$. Here the use of the YFMF variables requires only the solution of the two equilibrium equations for CO_2 and H_2O; NaCl is assumed to reside in the liquid phase only, hence $\lambda^{l,sc} = 1$. Figures 7a and 7b show the YFMF values for CO_2 and H_2O in the vapor phase. Very quickly after the CO_2 concentration rises above the value that can be absorbed in liquid, almost all the CO_2 goes into the vapor phase. On the other hand the H_2O solubility in the vapor is small, and only a small fraction goes into the vapor. PCMF values are shown in Figures 7c and 7d. The salting out effect on $x_{c,l}$ is apparent; as the salt molality increases in Figure 7d to its saturation limit, the CO_2 concentration decreases in Figure 7c. The effect on the smaller $x_{w,v}$ is weaker. These values are obtained from equation (11). Figure 7e shows the PMFs Λ^l and Λ^v calculated from equation (5). Their near linearity reflects the predominant $CO_2(H_2O)$ content of the vapor(liquid); Λ^v increases as Z_c while Λ^l decreases as $Z_w = 1 - Z_{sc} - Z_c$, both in a near-linear fashion.

5. Summary

[58] Reservoir calculations for CO_2 storage in brine aquifers encounter conditions that range from nearly pure supercritical CO_2 vapor along with residual solid salt; near

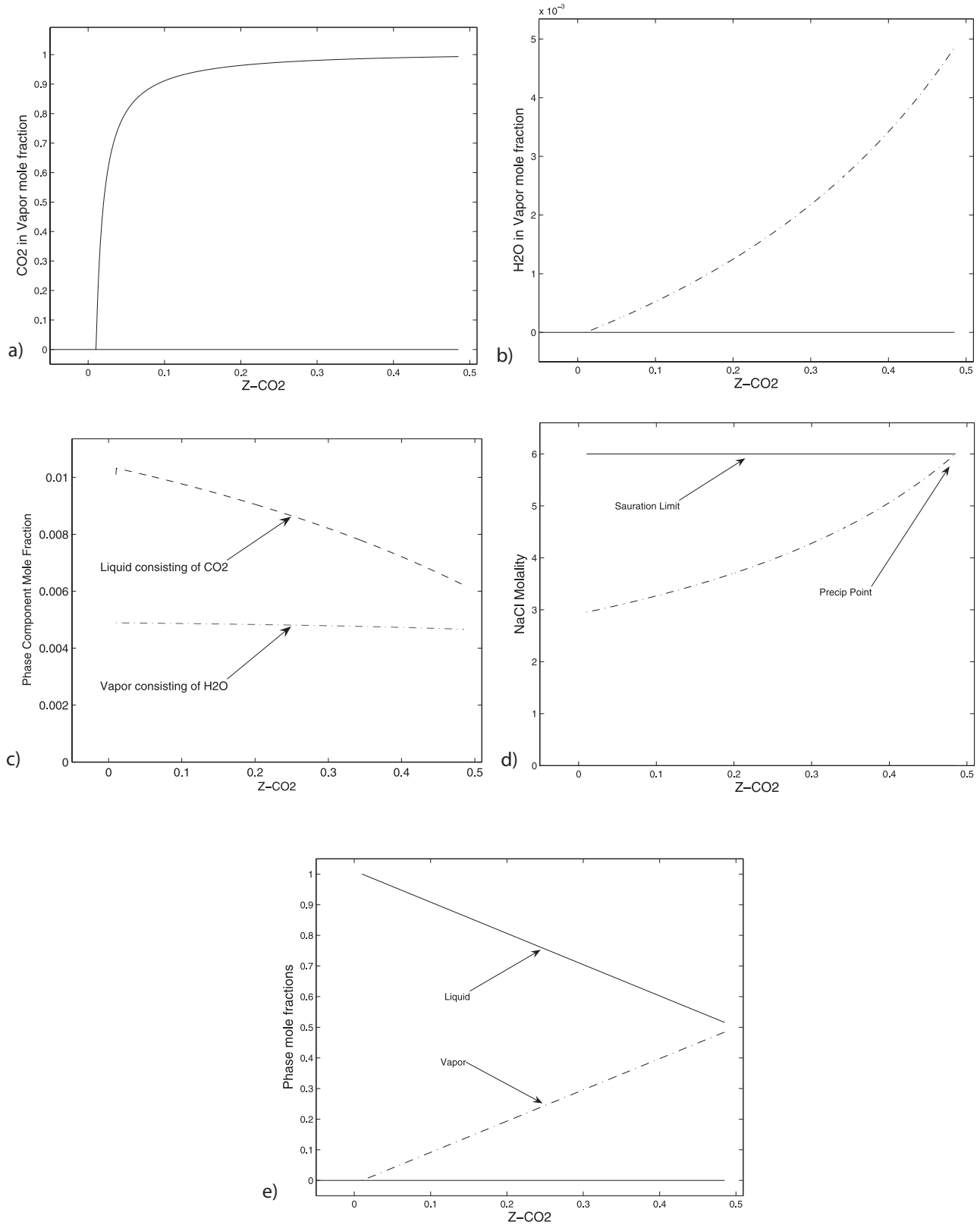

Figure 7. Results for the two-phase region. The YFMF fractions of (a) CO_2 and (b) H_2O in the vapor phase. (c) PCMFs for the fraction of the liquid phase consisting of CO_2 and of the vapor phase consisting of H_2O. (d) NaCl liquid molality with its saturation limit indicated. (e) Liquid and vapor PMFs.

the injection point, to a region of solid salt, carbonated brine, and CO_2 rich vapor; to a two-phase region of the carbonated brine and CO_2 rich vapor; and finally a front region of (carbonated) brine alone. Reservoir simulation transports CO_2 outward from the injection point resulting in a decline in CO_2 concentration that in turn is responsible for the phase succession. A flash calculation that supports CO_2 storage in brine aquifers must deal with all these phase configurations.

[59] If the number of phases equals the number of components, the equilibrium constraints alone determine the mole fractions within each phase; only the amount of each phase depends on the component inputs, and in particular, the boundaries of this phase region in the space of component inputs are easy to locate. This is the case for the dew and precipitation points in the CO_2 storage calculation.

[60] If each of the phases is not saturated in all of its components, then the mole fractions within the phases depend on the component inputs. It turns out that the mole fractions of a component in each phase, i.e., the yield factor mole fractions, provide variables that relate the phase component mole fractions to the component input mole fractions. With these variables equilibrium constraints depend on the component inputs, while at the same time they alone provide a complete set of equations for the flash calculation even when the number of phases and the number of components are not equal. This is the case for the brine-vapor system where the CO_2 solubility depends on the brine's salinity.

[61] Unlike previous calculations [*Pollack et al.*, 1988; *Søreide and Whitson*, 1992; *Pruess et al.*, 2004] we see the three effects of evaporation: (a) increase of brine salinity leading to reduction of CO_2 dissolution, (b) precipitation of salt from the brine, and (c) the no liquid region where any water is in the vapor.

[62] Finally, *Prevost et al.* [2004] found that this approach is fast enough to permit practical reservoir simulations, where the flash calculation must be repeated at each grid point at each time step and for every iteration.

Appendix A: Notation

[63] Our notation conventions include Latin subscripts or superscripts for components; Greek for phases. The number of moles of a component i in phase α is n_i^α; of component i in the flash chamber, n_i; of phase α in the flash chamber, n^α; a superscript in the denominator is demoted to a subscript in the result, $x_{i\alpha} = n_i^\alpha/n^\alpha$. We follow an analogous convention for subscripts in denominators. All intended sums are explicit; there is no implicit sum over repeated indices.

[64] Indices are necessary to specify calculation, but they can obscure relationships. We use Z to describe the set $\{Z_i\}$ of Z_i for all the components; when it makes sense Z can also denote the column vector of all the Z_i. In the same vein x_α denotes the set $\{x_{i\alpha}\}$ for all i. By removing subscripts and superscripts we hope to better communicate our relationship expressions; indices are used to specify a process of calculation.

[65] **Acknowledgments.** This work is supported in part by a grant from BP and Ford to Princeton University. This support is most gratefully acknowledged. Special thanks to Zhenhao Duan (University of California, San Diego) for providing us with his program to compute CO_2 solubility in brine, to George Scherer (Princeton University) for many helpful discussions and his thorough review of the manuscript and Jane Soohoo (Princeton University) for her efforts in preparation of the manuscript.

References

Castier, M., P. Rasmussen, and A. Fredenslund (1989), Calculation of simultaneous chemical and phase equilibrium in nonideal systems, *Chem. Eng. Sci.*, *44*(2), 237–248.

Duan, Z., and R. Sun (2003), An improved model calculating CO_2 solubility in pure water and aqueous *NaCl* solutions from 273 to 533 K and from 0 to 2000 bar, *Chem. Geol.*, *193*(3–4), 257–271.

Firoozabadi, A. (1999), *Thermodynamics of Hydrocarbon Reservoirs*, McGraw-Hill, New York.

Nghiem, L. X. K. Aziz, and Y. K. Li (1983), A robust iterative method for flash calculations using the Soave-Redlich-Kwong or the Peng-Robinson equation of state, *SPE J.*, *23*, 727–742.

Pollack, N. R., R. M. Enick, D. J. Mangone, and B. I. Morsi (1988), Effect of an aqueous phase on CO_2/tetradecane and CO_2/Maljamar-crude-oil systems, *SPE Reservoir Eng.*, *3*(2), 533–541.

Prausnitz, J. M., R. N. Lichtenthaler, and E. G. de Azevedo (1999), *Molecular Thermodynamics of Fluid Phase Equilibrium*, Prentice-Hall, Upper Saddle River, N. J.

Prevost, J. H., R. Fuller, A. S. Altevogt, R. Bruant, and G. Scherer (2004), Numerical modeling of carbon dioxide injection and transport in deep saline aquifers, paper presented at Seventh International Conference on Greenhouse Gas Control Technology, Univ. of Regina, Vancouver, B. C., Canada, 5–9 Sept.

Pruess, K., J. Garcia, T. Kovscek, C. Oldenburg, J. Rutqvist, C. Steefel, and T. Xu (2004), Code intercomparison builds confidence in numerical simulation models for geologic disposal of CO_2, *Energy*, *29*(9–10), 1431–1444.

Redlich, O., and J. Kwong (1949), On the thermodynamics of solutions. V. An equation of state. Fugacities of gaseous solutions, *Chem. Rev.*, *44*, 233–244.

Smith, J. M., H. C. Van Ness, and M. M. Abbott (1996), *Introduction to Chemical Engineering Thermodynamics*, 5th ed., McGraw-Hill, New York.

Søreide, I., and C. Whitson (1992), Peng-Robinson predictions for hydrocarbons, CO_2, N_2, and H_2S with pure water and *NaCl* brine, *Fluid Phase Equilibria*, *77*, 217–240.

Spycher, N., and K. Pruess (2005), CO_2-H_2O mixtures in the geological sequestration of CO_2. II. Partitioning in chloride brines at 12 to 100°C and up to 600 bar, *Geochim. Cosmochim. Acta*, *69*(13), 3309–3320.

Spycher, N., K. Pruess, and J. Ennis-King (2003), CO_2-H_2O mixtures in the geological sequestration of CO_2. I. Assessment and calculation of mutual solubilities from 12 to 100°C and up to 600 bar, *Geochim. Cosmochim. Acta*, *67*(16), 3015–3031.

Young, L. C., and R. E. Stephenson (1983), A generalized compositional approach for reservoir simulations, *SPE J.*, *23*, 727–742.

R. C. Fuller and J. H. Prevost, Department of Civil and Environmental Engineering, Princeton University, Princeton, NJ 08544, USA. (rcfuller@princeton.edu)

M. Piri, Department of Chemical and Petroleum Engineering, University of Wyoming, Department 3295, 1000 E. University Ave., Laramie, WY 82071-2000, USA. (mpiri@uwyo.edu)